PROCEEDINGS OF SCIENCE

Addressing the Impact of Solar Modulation Systematic Uncertainties on Cosmic-Ray Propagation Models

Isabelle John[a,b,*] **and Alessandro Cuoco**[a,b]

[a] *Dipartimento di Fisica, Università degli Studi di Torino, via P. Giuria, 1 10125 Torino, Italy*

[b] *INFN – Istituto Nazionale di Fisica Nucleare, Sezione di Torino, via P. Giuria 1, 10125 Torino, Italy*

E-mail: isabelle.john@unito.it, alessandro.cuoco@unito.it

While remarkable progress has been made to understand the propagation of cosmic rays, a variety of astrophysical uncertainties persists. At energies below about 20 GeV, the cosmic-ray flux is significantly modulated by solar activity, a process that is not precisely understood. Using the recently published AMS-02 data for the time-dependent cosmic-ray fluxes, we study the effects of solar modulation using force-field and extended force-field models and derive improved cosmic-ray propagation models. We find that simple solar modulation models are likely to underestimate the complexity of comic-ray propagation in the solar system and present limitations in describing the time-dependent fluxes consistently.

39th International Cosmic Ray Conference (ICRC2025)
15–24 July 2025
Geneva, Switzerland

*Speaker

PoS(ICRC2025)1304

1. Introduction

The local flux of cosmic rays is strongly shaped by the activity of the Sun. A combination of the heliospheric magnetic field and solar winds significantly suppresses the cosmic-ray flux below rigidities of $\sim$ 50 GV, referred to as solar modulation. Due to their complexity, the precise mechanisms of this process are not exactly understood. However, a detailed knowledge of the cosmic-ray fluxes is crucial to understand the origin of cosmic rays as well as the processes governing their propagation throughout the Galaxy and solar system. Additionally, an accurate understanding and modelling of the cosmic-ray fluxes is necessary to search for unexpected or exotic components in the cosmic-ray fluxes, for example from dark matter.

A variety of models has been developed to calculate the modulation of the cosmic-ray fluxes. Often, solar modulation is approximated by a force-field potential [1], which is however known to be insufficient at capturing the complexity of processes. Many extensions and modifications of the force-field model exist, which can take into account the time-, charge-, and rigidity dependence of solar modulation (see e.g. [2–5]), as well as models that use numerical codes to models cosmic-ray propagation in the heliosphere such as HelMod [6].

The modulation of the cosmic-ray fluxes is further characterised by the varying activity of the Sun over its 11-year cycle, peaking during the reversal of its magnetic field polarity. During periods of high solar activity, the flux is stronger suppressed than during periods of lower activity. Recently, AMS-02 has released time-dependent data for many cosmic-ray nuclei over a full solar cycle. Crucially, AMS-02 also provides the time-dependent data for antiprotons, which, due to their negative charge, are affected differently by solar modulation than protons and other positively charged nuclei. The high statistical precision of the data allows for a detailed study of the dependence of the cosmic-ray fluxes on solar activity, as this is not only expected to change the intensity of the cosmic-ray fluxes but may also affect the heliospheric propagation processes, which can result in different dependences on the charge and rigidity of the cosmic-ray nuclei. In this work, we make use of the time-dependent fluxes to investigate our understanding and modelling of solar modulation, and their underlying systematic uncertainties.

2. Cosmic-Ray Data Selection

AMS-02 provides time-dependent data for antiprotons and protons below $\sim$ 41 GV [7], as well as for cosmic-ray nuclei for Helium, Lithium, Beryllium, Boron, Carbon, Nitrogen, and Oxygen below $\sim$ 60 GV [8], spanning over a full solar cycle from May 2011 to November 2022 (solar cycle 24). We include the datasets for all these nuclei, except for Lithium and Beryllium, due to their large uncertainties in production cross sections [9] as well as the time-dependent Boron-to-Helium ratio [8]. We also take into account the time-dependent Helium-3-to-Helium-4 ratio from AMS-02 [10].

For a more complete fit, we also include data above the rigidities provided by the time-dependent datasets. Since the effects of time-dependence of solar modulation are small at these higher rigidities we use a fixed dataset, namely the AMS-02 7-years dataset [11] including data for protons, antiproton-to-proton ratio, Boron-to-Carbon ratio, Helium, Carbon, Oxygen, and Nitrogen, as well as the proton data from CALET [12], the Helium data from DAMPE [13], and the Boron-

to-Carbon ratio from DAMPE [14]. Additionally, we include the data from Voyager, which has measured the unmodulated LIS fluxes for protons and Helium outside the heliosphere at rigidities below ~ 1 GV [15].

For our analysis, we select data in the time range from May 2011 until April 2021, since not all the time-dependent AMS-02 datasets provide data in the full solar cycle range. Due to the change in solar activity, we further divide this time range into 3 periods, corresponding to a few months before the maximum of solar activity from May 2011 to November 2012 (Bartels rotations 2426 to 2446), the period during the maximum roughly from December 2012 to November 2015 (Bartels rotations 2447 to 2487), and after the maximum from December 2015 to April 2021 (Bartels rotations 2488 to 2560). Correspondingly, we refer to our 3 fit ranges as `preMAX`, `MAX` and `postMAX`.

3. Modelling Cosmic-Ray Propagation and Solar Modulation

We build our analysis on the cosmic-ray modelling framework developed in previous works [16–19]. This is based on the numerical cosmic-ray propagation code `GALPROP` [20, 21] that takes into account a variety of processes such as cosmic-ray injection, diffusion, convection, energy losses and re-acceleration. In order to fit over the complex multi-dimensional parameter space, we use MultiNest [22]. Our free parameters include for example various parameters for cosmic-ray injection, composition and diffusion (see References above for more details), as well as several solar-modulation specific parameters.

To study the impact of the chosen solar modulation model, we carry out our analysis for two different solar modulation models: (1) the simple and widely used force-field potential [1] and (2) an extended force-field potential [5] that allows for a rigidity dependence of the solar modulation potential.

The force-field potential relates the locally measured flux, $\Phi_{\rm loc}$, to the flux in the local interstellar medium (LIS), $\Phi_{\rm LIS}$, through

$$\Phi_{\rm loc}\left(E\right) = \Phi_{\rm LIS}\left(E + \phi Z/A\right) \times \frac{E \times \left(E + 2m_p\right)}{\left(E + \phi Z/A\right)\left(E + \phi Z/A + 2m_p\right)}, \tag{1}$$

where E is the kinetic energy per nucleon, Z and A charge and mass number of the nuclei, m_p the nucleon mass, and ϕ the solar modulation potential. Our fit includes two free parameters, ϕ_p for positively charged cosmic rays, and $\phi_{\bar{p}}$ for negatively charged cosmic rays (antiprotons).

The extended model modifies the force-field potential by introducing a dependence on the rigidity R, defined by

$$\phi_{\rm Ext}\left(R\right) = \phi_l + \left(\frac{\phi_h - \phi_l}{1 + \exp\left(-R + R_b\right)}\right), \tag{2}$$

where ϕ_l and ϕ_h are the modulation potential at low and high rigidities, respectively, separated by the break R_b. In our fit, we include 5 free parameter to describe the extended model: a low and high potential for positively and negatively charged cosmic rays, respectively, ($\phi_{l,p}$, $\phi_{h,p}$, $\phi_{l,\bar{p}}$, $\phi_{h,\bar{p}}$), while the break R_b applies to both negatively and positively charged cosmic rays.

	Force-Field Potential			Extended Model		
	preMAX	MAX	postMAX	preMAX	MAX	postMAX
ϕ_p [GV]	0.52	0.67	0.31	–	–	–
$\phi_{\bar{p}}$ [GV]	0.59	0.75	0.54	–	–	–
$\phi_{l,p}$ [GV]	–	–	–	0.52	0.67	0.31
$\phi_{h,p}$ [GV]	–	–	–	0.50	0.60	0.28
$\phi_{l,\bar{p}}$ [GV]	–	–	–	0.82	1.02	0.81
$\phi_{h,\bar{p}}$ [GV]	–	–	–	0.34	0.47	0.27
R_b [GV]	–	–	–	4.86	5.03	4.64

Table 1: Best-fit solar modulation parameters for the fits with the force-field potential (ϕ_p, $\phi_{\bar{p}}$) and the extended model ($\phi_{l,p}$, $\phi_{h,p}$, $\phi_{l,\bar{p}}$, $\phi_{h,\bar{p}}$, R_b) for the 3 time periods.

Since the processes causing solar modulation vary throughout the solar cycle, we perform separate fits to our 3 time periods defined above (preMAX, MAX and postMAX), for each solar modulation model. This allows us to test each model for different configurations of solar activity.

4. Results and Discussion

Figure 1 shows the cosmic-ray fluxes from our fits for protons (left panels) and antiprotons (right panels), for the force-field potential (top panels) and extended model (bottom panels). The fluxes for the different preMAX, MAX and postMAX periods are given in shades of orange, blue and burgundy, respectively. For each period, the LIS flux is given in dashed, and the modulated flux in solid lines. The time-dependent AMS-02 data is displayed with triangular markers, while the total time-independent AMS-02 data at energies above $\sim$ 40 GV is shown in gray circle markers. The bottom of each plot also shows the residuals of the modulated fluxes to each dataset. Generally, the extended model gives a better fit to the data than the force-field potential, indicating that the additional degrees of freedom introduced in the model are necessary to describe the complexity of solar modulation.

For both solar modulation models, the proton LIS fluxes display some differences, especially above $\sim$ 3 GV. This points towards some inconsistencies and difficulties at reconciling solar modulation, as all three LISs should be exactly the same and uneffected by solar activity. This means that the derived solar modulation potentials and underlying propagation models include some additional systematic uncertainties. The discrepancies in the force-field cases are larger than in the extended model, which indicates that the additional degrees of freedom introduced in the extended model may be able to address some of these uncertainties.

The antiproton LIS fluxes are consistent in both solar modulation cases. It is noticeable that the excess in the antiproton flux at around tens of GV [23, 24] is reduced in the extended model, stressing the importance of a precise understanding of cosmic-ray processes and systematic uncertainties [25].

In Table 1 we summarise the solar modulation parameters over the 3 solar activity periods for the force-field potential and extended model. As expected, the potentials are largest during the MAX phase when solar activity is strongest, and decrease before and after the maximum for periods of

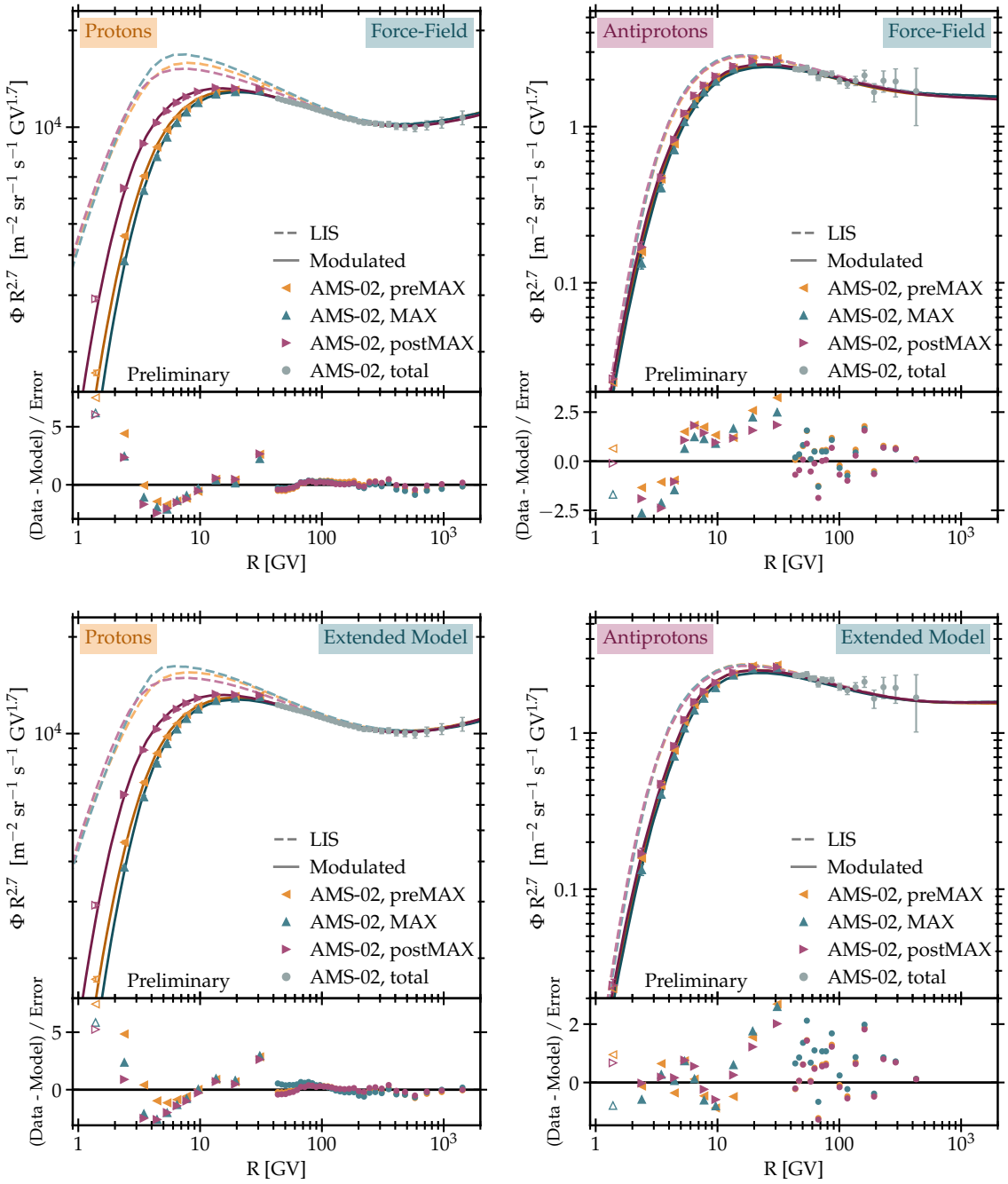

Figure 1: The cosmic-ray proton (left panels) and antiproton (right panels) fluxes against rigidity using the force-field approximation (top panels) and extended force-field model (bottom panels), for the `preMAX`, `MAX` and `postMAX` periods, given in shades of orange, blue and burgundy, respectively, for the LIS (dashed lines) and modulated fluxes (solid lines), compared to the time-dependent AMS-02 data (triangular markers) and the total AMS-02 flux at energies above ~ 40 GV (circular markers). The lower panels in each plot show the residuals, i.e. (Data - Model) / Error. Empty markers correspond to data points not included in the fit.

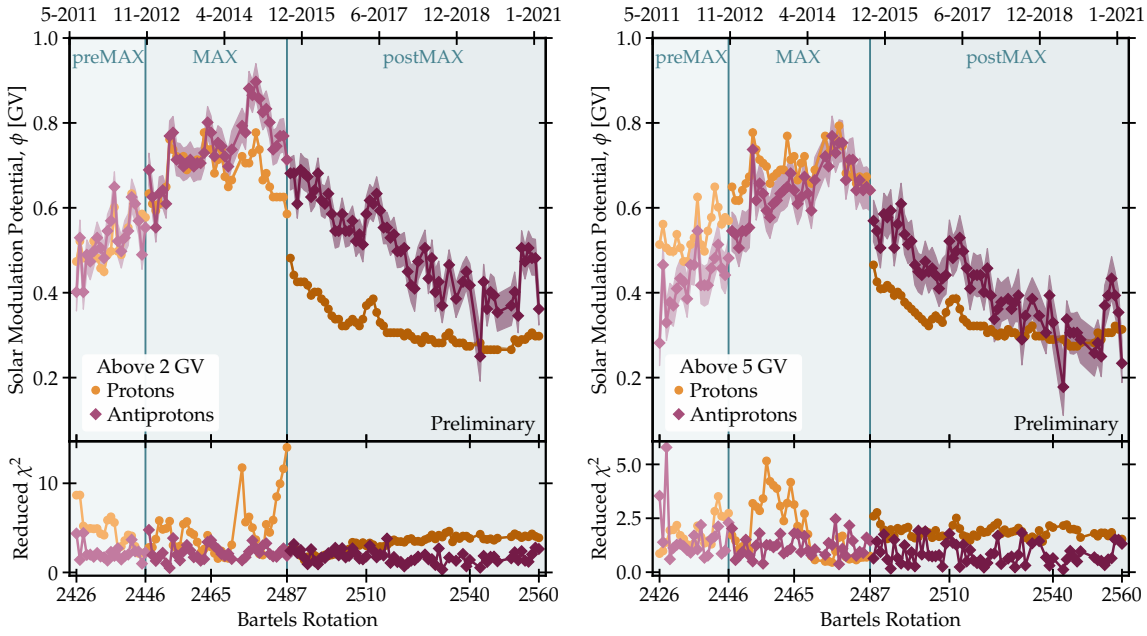

Figure 2: The solar modulation potential for each Bartels rotation. For the LIS obtained from our force-field fit for each of the 3 time periods, for protons (orange circle markers) and antiprotons (burgundy diamond markers). The left panel calculates the potential including all rigidities above 2 GV (as per our propagation model fit range), while the right panel only includes rigidities above 5 GV, motivated by the rigidity break in the extended model.

lower solar activity. Differences are observed between the potentials for protons (representatively for positively charged nuclei) and antiprotons (for negatively charged nuclei), as expected from the dependence of the polarity of the heliospheric magnetic field on charged particles.

In the extended model, the potential for antiprotons below the break ($\phi_{l,\bar{p}}$) is significantly larger than the potential above the break ($\phi_{h,\bar{p}}$). For protons both potentials are consistent, with only a moderate difference during the `MAX` phase. This seems to indicate that the force-field approximation for solar modulation works best during periods of lower solar activity, which is expected. A more complex treatment of solar modulation may be required instead for antiprotons. The rigidity break in the extended model, hence mostly driven by the antiproton flux, appears at around $\sim 4.6 - 5.0$ GV with good consistency across the 3 periods, suggesting that the force-field potential becomes inadequate below this rigidity.

Figure 2 shows the change in the solar modulation potential over time, calculated at each Bartels rotation, for the force-field model. Protons are shown in orange shades and circle markers, while antiprotons are shown in burgundy shades and diamond markers. The shaded bands indicate the 1σ uncertainty. In each of the 3 periods, we use the LIS obtained from the fit to the time-dependent AMS-02 data of that period. In the left panel, the modulation potential is calculated over the full range of rigidities chosen in the fitting procedure, starting from 2 GV. In the right panel, the modulation potential only includes rigidities above 5 GV, motivated by the preference of a break at roughly 5 GV in the extended model, which indicates a worsening of the force-field approximation below this rigidity. The bottom panels show the reduced χ^2 of the solar modulation potential with

respect to the time-dependent AMS-02 proton or antiproton data, respectively. They show a good agreement across all periods – note however the inconsistencies in the LIS fluxes as seen in Figure 1.

While for protons the modulation potential is roughly consistent in both rigidity cuts – as is expected from Table 1, where the extended model does not show a strong difference below and above the break for protons – the potential for antiprotons is lower by about 15 – 20% for rigidities above 5 GV. This is consistent with the observations from the extended model, preferring a high modulation potential for antiprotons below the break, but a lower potential above, closer to the proton potential. Note that we do not provide such a figure of the time-dependent potential for the extended model LIS, as the potential in this case is more complex due to its rigidity dependence.

5. Conclusions

Throughout our analysis we find that a simple description of solar modulation by a force-field potential, or even modified force-field potential with additional parameters, has difficulties in capturing the complexity of solar modulation and in building a coherent picture. We investigate the solar modulation potential separately for 3 periods of time and find moderate inconsistencies between the resulting LIS fluxes, for both the force-field and extended solar modulation models. However, the extended model highlights some shortcomings of the force-field model below $\sim$ 5 GV, especially for antiprotons. Additional analysis is needed to gain a more in-depth understanding of these crucial systematic uncertainties, and to disentangle the impact of solar modulation on the local cosmic-ray fluxes from other processes, such as re-acceleration or solar system specific diffusion, which shape the lower energy tail of the flux.

Further analysis and conclusions will be provided in the future publications.

Acknowledgements

IJ and AC acknowledge support from the Research grant TAsP (Theoretical Astroparticle Physics) funded by INFN, and Research grant "Addressing systematic uncertainties in searches for dark matter", Grant No. 2022F2843L, CUP D53D23002580006 funded by the Italian Ministry of University and Research (MUR).

References

[1] L. J. Gleeson and W. I. Axford, ApJ **154**, 1011 (1968).

[2] I. Cholis, D. Hooper, and T. Linden, JCAP **10**, 051 (2022), arXiv:2007.00669 [astro-ph.HE] .

[3] M. Kuhlen and P. Mertsch, Phys. Rev. Lett. **123**, 251104 (2019), arXiv:1909.01154 [astro-ph.HE] .

[4] W.-C. Long and J. Wu, Phys. Rev. D **109**, 083009 (2024), arXiv:2403.20038 [astro-ph.SR] .

[5] C.-R. Zhu, Astrophys. J. **975**, 270 (2024), arXiv:2409.18389 [astro-ph.HE] .

[6] M. J. Boschini, S. Della Torre, M. Gervasi, G. La Vacca, and P. G. Rancoita, Advances in Space Research **70**, 2649 (2022).

[7] M. Aguilar *et al.* (AMS), Phys. Rev. Lett. **134**, 051002 (2025).

[8] M. Aguilar *et al.* (AMS), Phys. Rev. Lett. **134**, 051001 (2025).

[9] D. Maurin *et al.*, (2025), arXiv:2503.16173 [astro-ph.HE] .

[10] M. Aguilar *et al.* (AMS), Phys. Rev. Lett. **132**, 261001 (2024).

[11] M. Aguilar *et al.* (AMS), Phys. Rept. **894**, 1 (2021).

[12] O. Adriani *et al.* (CALET), Phys. Rev. Lett. **129**, 101102 (2022), arXiv:2209.01302 [astro-ph.HE] .

[13] F. Alemanno *et al.*, Phys. Rev. Lett. **126**, 201102 (2021), arXiv:2105.09073 [astro-ph.HE] .

[14] F. Alemanno *et al.* (DAMPE), Sci. Bull. **67**, 2162 (2022), arXiv:2210.08833 [astro-ph.HE] .

[15] E. C. Stone, A. C. Cummings, F. B. McDonald, B. C. Heikkila, N. Lal, and W. R. Webber, Science **341**, 1236408 (2013).

[16] A. Cuoco, J. Heisig, L. Klamt, M. Korsmeier, and M. Krämer, Phys. Rev. D **99**, 103014 (2019), arXiv:1903.01472 [astro-ph.HE] .

[17] M. Korsmeier and A. Cuoco, Phys. Rev. D **103**, 103016 (2021), arXiv:2103.09824 [astro-ph.HE] .

[18] M. Korsmeier and A. Cuoco, Phys. Rev. D **105**, 103033 (2022), arXiv:2112.08381 [astro-ph.HE] .

[19] M. Di Mauro, M. Korsmeier, and A. Cuoco, Phys. Rev. D **109**, 123003 (2024), arXiv:2311.17150 [astro-ph.HE] .

[20] A. W. Strong and I. V. Moskalenko, Astrophys. J. **509**, 212 (1998), arXiv:astro-ph/9807150 .

[21] A. W. Strong, (2015), arXiv:1507.05020 [astro-ph.HE] .

[22] F. Feroz, M. P. Hobson, and M. Bridges, Mon. Not. Roy. Astron. Soc. **398**, 1601 (2009), arXiv:0809.3437 [astro-ph] .

[23] M. Cirelli, D. Gaggero, G. Giesen, M. Taoso, and A. Urbano, JCAP **12**, 045 (2014), arXiv:1407.2173 [hep-ph] .

[24] A. Cuoco, M. Krämer, and M. Korsmeier, Phys. Rev. Lett. **118**, 191102 (2017), arXiv:1610.03071 [astro-ph.HE] .

[25] K.-K. Duan, X. Wang, W.-H. Li, Z.-H. Xu, Y.-L. S. Tsai, and Y.-Z. Fan, (2025), arXiv:2506.13352 [astro-ph.CO] .

PoS(ICRC2025)1304